

# Combination of automatic non-rigid and landmark based registration: the best of both worlds

Bernd Fischer and Jan Modersitzki

Institute of Mathematics, University of Lübeck,

Wallstraße 40, 23560 Lübeck, Germany

E-Mail: {fischer,modersitzki}@math.uni-luebeck.de

## Abstract

In particular in medical imaging, registration schemes are known to be valuable tools in various settings, like, e.g., the comparison of pre- and post biopsy images. The currently available schemes can roughly be divided in two classes: landmark based and intensity based registration schemes. In this paper, we present a rigorous mathematical framework for combining these two techniques, in order to benefit from the advantages of both strategies.

Intensity based approaches aim to match images by minimizing an appropriate distance measure, like, e.g., the  $L_2$ -norm of the difference image or the mutual information of the two images. These techniques are generally full automatic and yield a good registration on the average. However, they may perform poorly for specific, important locations like anatomical landmarks. On the opposite, landmark based registration techniques are designed to accurately match user specified landmarks. A drawback of landmark based registration is the fact that the intensities of the images are completely neglected. Consequently, the registration result away from the landmarks may be very poor.

Here, we propose a mathematical framework for combining any distance measure based registration with landmark information. We also present a general numerical procedure for computing the wanted transformation as well as a particular implementation for a specific distance measure based registration technique. The general procedure computes a displacement field which is mathematically guaranteed to produce a one-to-one match between given landmarks and at the same time to minimize an intensity based measure for the remaining parts of the images. The properties of the new scheme are demonstrated for a variety of examples.

It is important to observe, that the presented novel technique for combining intensity driven and landmark based approaches is independent on the two main building blocks.

**Keywords:** Image processing, image registration, elastic-registration, landmark registration

## 1 INTRODUCTION

Image registration is an often encountered problem in many application areas like, for example, geophysics, medicine, and robotics. For an overview we refer to [6, 15, 19, 14], and references therein. In the last two decades, computerized image registration has played an increasingly important role in particular in medical imaging. Registered images are now used routinely in a multitude of different applications, such as the treatment verification of

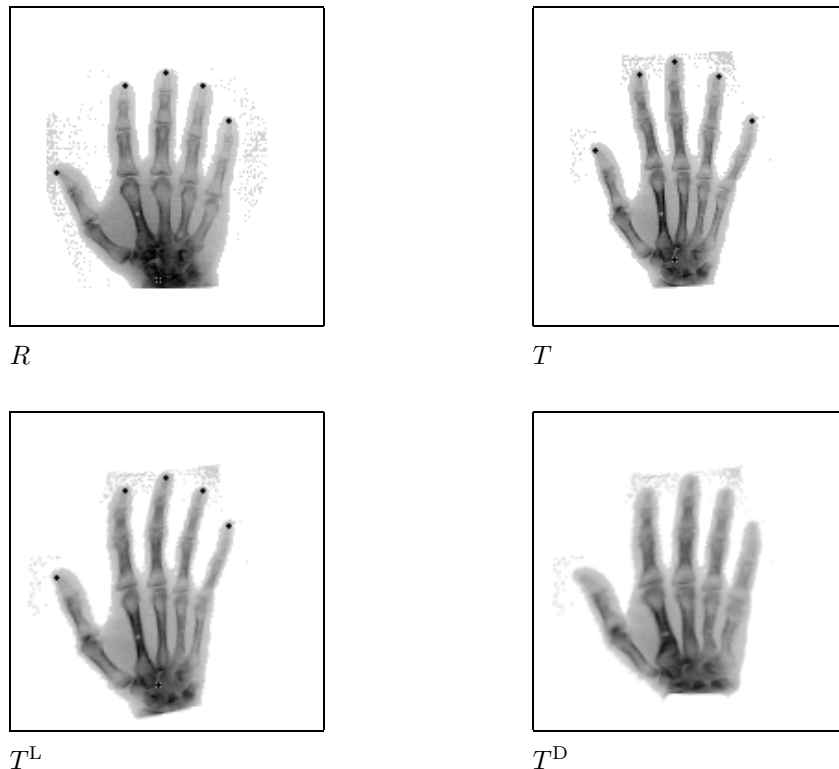


Figure 1: Registration results for X-rays of a human hand (images from Y. AMIT [1]): TOP LEFT: reference  $R$  with 6 landmarks, TOP RIGHT: template  $T$  with 6 corresponding landmarks, BOTTOM LEFT: template  $T^L$  after landmark based registration, and BOTTOM RIGHT: template  $T^D$  after distance measure based registration.

pre- and post-intervention images and the time evolution of an agent injection subject to patient motion. They are also useful to take full advantage of the complementary information coming from multimodal imagery, like, for example, computer tomography (CT) and magnetic resonance imaging (MRI).

Two fundamental approaches are popular in today's image registration. One is based on the detection of a number of outstanding points, the so-called *landmarks*, and the second one is based on the minimization of an appropriate chosen *distance measure*. In the next example (see Fig. 1) we illustrate the properties of these two approaches. Given are two images, typically called the *reference*  $R$  and the *template*  $T$ . The goal is to find a spatial transformation, such that the deformed template matches the reference image. For the landmark based registration, we have chosen six landmarks and computed the thin-plate-spline with respect to these points, i.e., a second order derivative based energy functional has been used as a regularizer (see  $T^L$ , Fig. 1, bottom left). As the distance based registration technique we have chosen the curvature matching scheme (see Section 3.1), a method which relies on a distance measure (for this example, the  $L_2$  distance) in combination with a second order derivative based regularizer (see  $T^D$ , Fig. 1, bottom right).

As it is apparent from the plots, we encounter a method inherent dilemma. Using a landmark based registration technique, we are able to guarantee a one-to-one match for the user defined landmarks. However, the overall registration is visually unpleasing, as

the scheme solely makes use of the landmarks. On the other hand, although the distance measure based approach produces visually pleasing results, there is no guarantee, that there is a one-to-one correspondence between the landmarks, as the scheme “does not know” about the landmarks.

In this paper, we propose a novel registration technique, which combines the concepts of landmark and automatic, non-rigid distance measure based approaches (CLD registration). Roughly spoken, the idea is to minimize a regularized distance measure subject to some interpolation constraints. It is important to note, that the presented technique does work for any (sensible) intensity measure, i.e., the user may choose his application dependent favorite intensity measure. Moreover, we present a fast and robust numerical scheme for the computation of the wanted minimizer. Here, the desired deformation is computed iteratively using an EULER-scheme for the first variation of the chosen objective functional. The deformations are restricted to fulfill the interpolation constraints. Consequently, the CLD registration guarantees that each intermediate iterate and in particular the final stationary solution do produce a one-to-one correspondence of the prescribed landmarks. At the same time the whole process is minimizing an intensity based measure for the remaining parts of the images. The computational overhead in our implementation introduced by the consideration of landmarks is negligible as compared to the conventional scheme without landmarks.

There are already some attempts in the literature to design registration schemes which are based on matching both landmark and intensity information; see, e.g., [12, 13]. This fact indicates the there is demand for a general solution of this interesting and timely question. However, they are all restricted to special functionals and are not as versatile as the proposed framework.

The paper is organized as follows. In Section 2, we introduce the basic ideas and the general mathematical setting. The ingredients of our new approach are introduced in detail in Section 3 and a numerical treatment is presented in Section 4. We conclude with some examples in Section 5.

## 2 BASIC IDEAS

In this section we set the mathematical framework and briefly introduce the landmark based and intensity driven approaches. Finally, we describe our new approach and discuss its basic ideas.

Let  $d \in \mathbb{N}$  denote the dimension of a spatial domain  $\Omega \subset \mathbb{R}^d$ , where without loss of generality, we assume  $\Omega = ]0, 1[^d$ . Furthermore, let  $R, T : \Omega \rightarrow \mathbb{R}$  denote the two images. Hence,  $T(x)$  denotes the intensity of the template at the spatial position  $x$ , where for ease of discussion we set  $R(x) = T(x) = 0$  for all  $x \notin \Omega$ . The overall goal is to find a *displacement*  $u$ ,  $u : \mathbb{R}^d \rightarrow \mathbb{R}^d$ , such that ideally  $T(x - u(x)) \approx R(x)$  for all  $x \in \Omega$ .

There are various ways of computing a suitable displacement  $u$ . Let us start with intensity driven approaches. Here, one attempts to minimize an appropriate functional. It typically has two building blocks. One of them computes *internal forces*, which are defined for the wanted displacement field itself, whereas the other one is responsible for *external forces*, which are computed from the image data. The internal forces are designed to keep the displacement field smooth during deformation, while the external forces are defined to obtain the desired registration result. It turns out that most of these schemes may be formulated in the following fashion; see, e.g. [10]. Find a displacement  $u : \mathbb{R}^d \rightarrow \mathbb{R}^d$ , such that

$$\mathcal{J}[u] := \mathcal{D}[R, T; u] + \alpha \mathcal{S}[u] = \min .$$

where  $\mathcal{D}$  represents a *distance measure* (external force) and  $\mathcal{S}$  determines the *smoothness* of  $u$  (internal force). The parameter  $\alpha$  may be used to control the strength of the smoothness of the displacement versus the similarity of the images. The second term  $\mathcal{S}$  is unavoidable. Arbitrary transformations may lead to cracks, foldings, or other unwanted deformations. From a mathematical point of view,  $\mathcal{S}$  may also be seen as a regularizing term introduced in order to rule out discontinuous and/or suboptimal solutions, having in mind that image registration is an ill-posed problem.

The actual choice of  $\mathcal{D}$  and  $\mathcal{S}$  depends on the application under consideration. Some of the most common choices will be discussed in Section 3.2. From a numerical point of view, it is desirable that  $\mathcal{D}$  and  $\mathcal{S}$  possess a GÂTEAUX-derivative. For this case, one may characterize a minimizer of  $\mathcal{J}$  as solution of the so-called EULER-LAGRANGE equations

$$f(x, u(x)) + \alpha \mathcal{A}[u](x) = 0, \quad x \in \Omega. \quad (1)$$

Here,  $f$  is related to the GÂTEAUX-derivative of the distance measure  $\mathcal{D}$  and the partial differential operator  $\mathcal{A}$  is related to the GÂTEAUX-derivative of the smoother  $\mathcal{S}$ , respectively. The above semi-linear partial differential equation allows for a fast and robust computation of the wanted minimizer; for details, we refer to [10, 16].

To solve the semi-linear EULER-LAGRANGE equations either a fixed-point type iteration scheme

$$\alpha \mathcal{A}[u^{(k+1)}](x) = -f(x, u^{(k)}(x)), \quad k \geq 0,$$

or a time-marching iteration

$$\partial_t u^{(k+1)}(x, t) = f(x, u^{(k)}(x, t)) + \alpha \mathcal{A}[u^{(k+1)}](x, t), \quad k \geq 0,$$

with  $u^{(0)}(x, 0) = 0$ , may be employed. The main work in each iteration is the solve for  $u^{(k+1)}$ , i.e., the solution of a linear partial differential equation. Here, we are using a finite-difference approximation of the equation followed by the application of an efficient solver for the resulting linear system of equations. As it turns out, the sparse linear systems do have a rich structure, which may be used to advantage. Here, specific implementations lead to overall schemes with complexity  $\mathcal{O}(N \log N)$  or even  $\mathcal{O}(N)$ , where  $N$  denotes the number of voxel. The actual complexity depends on the chosen smoother  $\mathcal{S}$ ; see [16].

Let us now briefly introduce the landmark based approach. To this end, let the landmarks  $r^j, t^j \in \mathbb{R}^d$ ,  $j = 1, \dots, m$ , be given. The idea is to find a smooth displacement  $u$  such that  $t^j$  is mapped onto  $r^j$ ,  $j = 1, \dots, m$ . Again, a regularizer  $\mathcal{S}$  is incorporated in order to ensure smoothness of the solution. Altogether, we end up with following scheme. Find a displacement  $u : \mathbb{R}^d \rightarrow \mathbb{R}^d$ , such that

$$\mathcal{S}[u] = \min \quad \text{subject to} \quad u(t^j) = t^j - r^j =: d^j, \quad j = 1, \dots, m. \quad (2)$$

As it is apparent, the distance between  $R$  and  $T$  is no longer part of the functional. The images enter into the scheme only through the landmarks. As for the distance measure based registration, we have two building blocks. The internal forces which control the smoothness of the wanted displacement and the external forces, which arise now from the locations of the landmarks.

As for the distance measure based approach, it is possible to provide necessary conditions for  $u$  to be a minimizer of (2) in terms of a partial differential equation. This time it is helpful to consider the point-evaluation functional  $\delta$ . With  $\delta_z[u] = u(z)$ , the interpolation constraints read  $\delta_{t^j}[u] - d^j = 0$ ,  $j = 1, \dots, m$ . Considering the LAGRANGE-functional

$$L[u, \lambda] := \mathcal{S}[u] + \sum_{j=1}^m \lambda_j (\delta_{t^j}[u] - d^j),$$

the wanted solution is characterized by

$$\mathcal{A}[u](x) + \sum_{j=1}^m \lambda_j \delta_{t^j}[u](x) = 0, \quad x \in \Omega, \quad (3)$$

$$\text{and } \delta_{t^j}[u] - d^j = 0, \quad j = 1, \dots, m. \quad (4)$$

where, again,  $\mathcal{A}$  is related to the GÂTEAUX-derivative of the smoother  $\mathcal{S}$ . For special choices of the smoother  $\mathcal{S}$ , it is actually possible to explicitly compute the solution of Eq. (3) in terms of fundamental solutions; for details, see [3, 17].

Having the outlined landmark and distance measure based approaches in mind, it is almost obvious how to combine them both to obtain the new CLD scheme. It can be thought of computing a displacement that minimizes the combination of a distance measure and a smoother while being guided by the landmark correspondences. Again, the internal forces are used to keep the displacement smooth, while the external forces are now a combination from landmark and intensity information. The mathematical description of the problem reads as follows. Find a displacement  $u : \mathbb{R}^d \rightarrow \mathbb{R}^d$ , such that

$$\left. \begin{aligned} \mathcal{J}[u] = \mathcal{D}[R, T; u] + \alpha \mathcal{S}[u] = \min \\ \text{subject to } u(t^j) = d^j = t^j - r^j, \quad j = 1, \dots, m. \end{aligned} \right\} \quad (5)$$

A minimizer is characterized by

$$f(x, u(x)) + \alpha \mathcal{A}[u](x) + \sum_{j=1}^m \lambda_j \delta_{t^j}[u](x) = 0, \quad x \in \Omega, \quad (6)$$

$$\text{and } \delta_{t^j}[u] - d^j = 0, \quad j = 1, \dots, m. \quad (7)$$

Observe, that equation (6) and (7) may be seen as a combination of the necessary condition for the pure intensity driven approach (1) and the landmark scheme (3), (4). This time, we have to solve a distributional, semi-linear partial differential equation. Though this task appears on the first glance quite tricky, the underlying numerics given in Section 4 are surprisingly easy and elegant. Their main building blocks are the well understood methods developed for the landmark and intensity registration algorithms, of course.

### 3 SOME DETAILS

Before we present our numerical scheme for the solution of (6) and (7), we discuss some important aspects of the regularization, the distance measure, and the landmark based registration in more detail.

#### 3.1 The regularizer

There exist various choices for the smoothing term  $\mathcal{S}$ . This is mainly motivated by the fact that particular applications demand for particular properties of the displacement field. In view of the need for fast numerical implementations, we concentrate on differentiable regularizer  $\mathcal{S}$ , i.e., functionals where the GÂTEAUX-derivative  $d\mathcal{S}[u; v]$ , given by

$$d\mathcal{S}[u; v] := \lim_{h \rightarrow 0} \frac{1}{h} (\mathcal{S}[u + hv] - \mathcal{S}[u]) = \int_{\Omega} \langle \mathcal{A}[u], v \rangle_{\mathbb{R}^d} dx,$$

exists. Here,  $\mathcal{A}$  denotes the associated linear partial differential operator. The most popular choices for intensity driven registration, the so-called *elastic* [5, 2], *fluid* [7, 4], *demon* [18], *diffusion* [9], and *curvature* [11] registration are based on regularizer which belong to this class. For a general treatment and the derivation of the different partial differential operators we refer to [16].

The numerical examples shown in Section 5 are based on the so-called curvature regularizer [11]

$$\mathcal{S}[u] = \mathcal{S}^{\text{curv}}[u] := \frac{1}{2} \sum_{\ell=1}^d \int_{\Omega} (\Delta u_{\ell})^2 dx.$$

Here, the associated partial differential operator

$$\mathcal{A}[u] = \mathcal{A}^{\text{curv}}[u] = (\Delta^2 u_1, \dots, \Delta^2 u_d)^{\top} \quad \text{with} \quad \Delta^2 u_{\ell} = \sum_{j,k=1}^d \partial_{x_j x_j x_k x_k} u_{\ell}$$

is nothing but the well-known biharmonic operator, which is rotationally invariant and decouples with respect to the spatial coordinates.

### 3.2 The distance measure

In the literature one may find various choices for the distance measure. Again, we concentrate on those measures  $\mathcal{D}$  which allow for differentiation, i.e., there exists a function  $f : \mathbb{R}^d \times \mathbb{R}^d \rightarrow \mathbb{R}^d$  with

$$\begin{aligned} d\mathcal{D}[R, T; u; v] &= \lim_{h \rightarrow 0} \frac{1}{h} (\mathcal{D}[R, T; u + hv] - \mathcal{D}[R, T; u]) \\ &= \int_{\Omega} \langle f(x, u(x)), v(x) \rangle_{\mathbb{R}^d} dx. \end{aligned}$$

Here and elsewhere,  $f$  is frequently called *force field*.

Probably the most popular choice for a distance measure, having this property, is provided by the so-called *sum of squared differences* (SSD)

$$\begin{aligned} \mathcal{D}[R, T; u] &= \mathcal{D}^{\text{SSD}}[R, T; u] \\ &:= \frac{1}{2} \|R - T(\cdot - u)\|_{L_2}^2 = \frac{1}{2} \int_{\Omega} (T(x - u(x)) - R(x))^2 dx. \end{aligned}$$

The associated force field looks like  $f(x, u(x)) = (R(x) - T(x - u(x))) \cdot \nabla T(x - u(x))$ . For this measure to be successful, one has to assume that the intensities of the two given images are comparable. Other distance measures, capable of dealing with multimodal images, like, e.g., mutual information [8, 20], are also under consideration.

### 3.3 The landmark registration

As pointed out in the introduction, depending on the smoother, the solution of the landmark based registration may be computed explicitly. Here, we will briefly outline the underlying mathematics as they will re-appear in our new scheme. The precise formulation of Eq. (3) for the  $\ell$ th component of the multivariate functions reads

$$\sum_{\nu=1}^d \left( \mathcal{A}_{\ell, \nu}[u_{\nu}] + \sum_{j=1}^m \lambda_j^{\ell} \delta_{t^j}[u_{\ell}] \right) = 0 \quad \text{and} \quad \delta_{t^j}[u_{\ell}] - d_{\ell}^j = 0, \quad j = 1, \dots, m.$$

Here,  $u = (u_1, \dots, u_d)^\top$ , the point evaluation function  $\delta$  is univariate, i.e.,  $\delta_{t^j}[u_\ell] = u_\ell(t^j) \in \mathbb{R}$ , and  $\mathcal{A}_{\ell,\nu}$  denotes the  $\ell$ th component of the operator  $\mathcal{A}$  acting on the  $\nu$ th component of  $u$ . For example, if  $\mathcal{S} = \mathcal{S}^{\text{curv}}$ , we have  $\mathcal{A}_{\ell,\nu} = \sum_{j,k=1}^d \partial_{x_j x_j x_k x_k}$  if  $\ell = \nu$  and  $\mathcal{A}_{\ell,\nu} = 0$  if  $\ell \neq \nu$ .

Let  $\rho^j$  denote the multivariate fundamental solution or Greens-functions of  $\mathcal{A}[\rho^j] = -\delta_{t^j}$ . Then the wanted solution can be written as

$$u = \sum_{\nu=1}^m \lambda_\nu \rho^\nu = \left( \sum_{\nu=1}^m \lambda_\nu^1 \rho_1^\nu, \dots, \sum_{\nu=1}^m \lambda_\nu^d \rho_d^\nu \right)^\top.$$

The free coefficients  $\lambda_\nu^\ell$  are determined by the interpolation constraints

$$\sum_{\nu=1}^m \lambda_\nu^\ell \rho_\ell^\nu(t^j) = d_\ell^j, \quad j = 1, \dots, m, \quad \ell = 1, \dots, d,$$

which may be written in compact notation as  $B^\ell \lambda^\ell = b^\ell$ , where

$$\begin{aligned} \lambda^\ell &:= (\lambda_1^\ell, \dots, \lambda_m^\ell)^\top \in \mathbb{R}^m, \\ B_{j,\nu}^\ell &:= [\rho_\ell^\nu(t^j)]_{j,\nu=1}^m \in \mathbb{R}^{m \times m}, \\ \text{and } b_j^\ell &:= (d_\ell^1, \dots, d_\ell^m)^\top \in \mathbb{R}^m. \end{aligned}$$

For various choices of  $\mathcal{S}$ , the Greens-functions are explicitly known. Often they are given in terms of a (univariate) radial basis function  $\hat{\rho}$  via  $\rho_\ell^\nu(x) = \hat{\rho}(\|x - x^{T,\nu}\|_{\mathbb{R}^d})$ . This is in particular the case, for the choice  $\mathcal{S} = \mathcal{S}^{\text{curv}}$ . Equipped with appropriate boundary conditions, this choice leads to the well-known thin-plate-splines.

## 4 A NUMERICAL SCHEME FOR CLD

In this section we comment on how to efficiently solve the characterizing equations (6) and (7) for the solution of the new CLD approach. To begin with, we compute the fundamental solutions or Greens-function  $\rho^j$  of

$$\alpha \mathcal{A}[\rho^j] = -\delta_{t^j}, \quad j = 1, \dots, m. \quad (8)$$

If  $w$  is the particular solution of

$$\alpha \mathcal{A}[w] = -f(\cdot, u(\cdot)), \quad (9)$$

then

$$u = w + \sum_{j=1}^m \lambda_j \rho^j = \left( w_1 + \sum_{j=1}^m \lambda_j^1 \rho_1^j, \dots, w_d + \sum_{j=1}^m \lambda_j^d \rho_d^j \right)^\top, \quad (10)$$

fulfills equation (6) for any choice of the coefficients  $\lambda_j^\ell$ . If in addition, the coefficients  $\lambda_j^\ell$  are chosen such that the interpolation conditions (7) are fulfilled,  $u$  (cf. (10)) is stationary for the functional  $\mathcal{J}$ , which is what we are looking for. Note, that the computation of the  $\lambda_j^\ell$  does involve the solution of an  $m \times m$  linear system with the coefficient matrix  $B^\ell$  introduced for landmark registration; see Section 3.3.

In the present form, the outlined computational scheme is not applicable. The problem is that the computation of  $w$  in (9) involves the knowledge of  $u$ . As already mentioned in Section 2, there exist two standard approaches for overcoming this problem. For the fixed-point type iteration, we start with an initial guess  $u^{(k)}$  fulfilling the interpolation

Table 1: Combined distance measure and landmark based registration algorithm CLD.

1. Initialize:
  - (a) Set  $k = 0$ ,  $u^{(k)} = 0$ .
  - (b) For  $j = 1, \dots, m$ , solve  $\alpha\mathcal{A}[\rho^j] = -\delta_{t^j}$ , end.
  - (c) Set  $B^\ell = [\rho_\ell^\nu(t^j)]_{j,\nu=1}^m$ .
2. Iterate:
  - (d) Compute  $f^{(k)}(x) = f(x, u^{(k)}, R, T)$ .
  - (e) Solve  $\alpha\mathcal{A}[w^{(k)}] = -f^{(k)}$ .
  - (f) For  $\ell = 1, \dots, d$ ,
    - (g) compute  $\lambda^\ell$  from  $B^\ell \lambda^\ell = b^\ell$ ,
    - (h) set  $b^\ell := [w_\ell(t^j) - t_\ell^j + r_\ell^j]_{j=1}^m$ ,
    - (i) compute  $\lambda^\ell$  from  $B^\ell \lambda^\ell = b^\ell$ ,
    - (j) set  $u_\ell^{(k+1)} = w_\ell^{(k)} + \sum_{j=1}^m \lambda_j^\ell \rho_\ell^j$ ,
    - (k) end.
    - (l)  $k \mapsto k + 1$
    - (m) stop, if converged.

constraints (7), solve  $\alpha\mathcal{A}[w^{(k+1)}] = -f(\cdot, u^{(k)}(\cdot))$ , and update  $u^{(k+1)} = w^{(k)} + \sum_{j=1}^m \lambda_j \rho^j$ . For a time-marching iteration, we make  $u$  (and hence  $w$ ) time-dependent, replace Eq. (6) by

$$\partial_t u = f(x, u(x)) + \alpha\mathcal{A}[u](x) + \sum_{j=1}^m \lambda_j \delta_{t^j}[u](x), \quad \text{for all } x \in \Omega, t \geq 0, \quad (11)$$

and solve for  $u$ . Note, if  $\partial_t w = f(\cdot, u(\cdot)) + \alpha\mathcal{A}[w]$ , then Eq. (11) is satisfied by  $u$  given by Eq. (10), since the  $\rho^j$ 's (cf. Eq. (8)) do not depend on time. Note that Eq. (11) is nothing but a gradient-flow towards a minimizer of the registration problem. If  $u$  becomes stationary,  $\partial_t u = 0$  and thus  $u$  is also a solution of Eq. (6).

The overall algorithm is summarized in Table 1. As a stopping rule we used a combination of the following three criteria,

$$\begin{aligned} \left\| R - T(\cdot - u^{(k)}) \right\|_{L_2(\Omega)} &\ll \left\| R - T(\cdot - u^{(0)}) \right\|_{L_2(\Omega)}, \\ \sum_{\ell=1}^d \left\| f_\ell^{(k)} \right\|_{L_2(\Omega)} &\ll 1, \quad \text{or} \\ \sum_{\ell=1}^d \left\| u_\ell^{(k)} \right\|_{L_2(\Omega)} &\ll 1, \end{aligned}$$

where  $\|\cdot\|_{L_2(\Omega)}$  is the  $L_2$ -norm.

Some comments are in order. The computation of the fundamental solution  $\rho^j$  (Table 1b) may be done once and forever, as they are independent of  $T$ ,  $R$ , and the iteration index  $k$ .

Actually, as outlined at the end of Section 3.3, the fundamental solutions are even explicitly known for various choices of the smoother  $\mathcal{S}$ . However, this issue is not critical for our implementation, as we do have competitive fast solvers for the partial differential equations anyway. In general, the most time consuming part in the iteration loop is the solve for  $w^{(k)}$ ; see, Table 1e. Here we employ a finite difference scheme, followed by a specifically designed direct solver for the resulting linear system of equations [16]. For example, for the partial differential equation associated with the curvature smoother, a proper use of the discrete cosine transformations leads to an  $\mathcal{O}(N \log N)$  direct scheme for the solution of the linear system [11]. Apart from the startup phase, the overhead connected to the CLD approach is the solution of  $d$  small  $m \times m$  linear systems for the parameter  $\lambda^l$  (Table 1i) and the update of  $u$  (Table 1j). It is worth noticing, that the partial differential equation (Table 1e) is identical to the one obtained by solving the registration problem without landmarks. In other words, existing codes can easily be modified to incorporate landmarks.

Finally, a few comments on pre-registration. To perform satisfactory, non-rigid registration schemes do need a good starting point. Therefore, in general, some sort of pre-registration has to be performed. Typically, an affine linear registration scheme is applied. However, as can be seen from the following examples, this strategy does not always work. If there are some landmarks available, we propose to use the image obtained by a plain landmark based registration as starting point for the non-rigid registration. As an outcome, in all our experiments, the non-rigid scheme did converge very rapidly to the wanted solution.

## 5 EXAMPLES

In this section we present three examples. Two of them are academic and are designed to show some special features of the CLD scheme as opposed to conventional schemes. We conclude with a more realistic example. For simplicity and comparison reasons, we used the distance measure  $\mathcal{D}^{\text{SSD}}$ , and the regularizer  $\mathcal{S}^{\text{curv}}$  in all examples.

### 5.1 Landmarks to improve the initial configuration

In the first example, the reference is a big gray square with two inner structures, a small white square and a triangle; cf. Fig. 2. The difference in the template is that the inner structures are moved to the bottom.

Apart from the reference and template, Fig. 2 displays four registration results. The first one (top right image) shows an intermediate result of a plain distance measure based registration. Here, the inner square is deformed to the triangle and the triangle in the template disappears. This process is completed after about 50 iterations. Note, since we have a dominating outer gray square this mis-registration cannot be avoided by performing an affine linear pre-registration, as this pre-registrations does not change the initial configuration at all.

The second registration (bottom left image) is the result of a plain landmark based registration. The eleven corners of the reference and template images are used as landmarks. Note that the displayed landmarks (black “+” on gray background) do not belong to the images. As it is apparent from this figure, the match of the inner structures is quite good, however, the edges of the outer gray square are deformed unacceptably.

The third registration (bottom middle image) is again a distance measure based registration. This time we used the outcome of the landmark based registration as a starting point. This guarantees a rough match of the inner and outer structures of the images. Here we

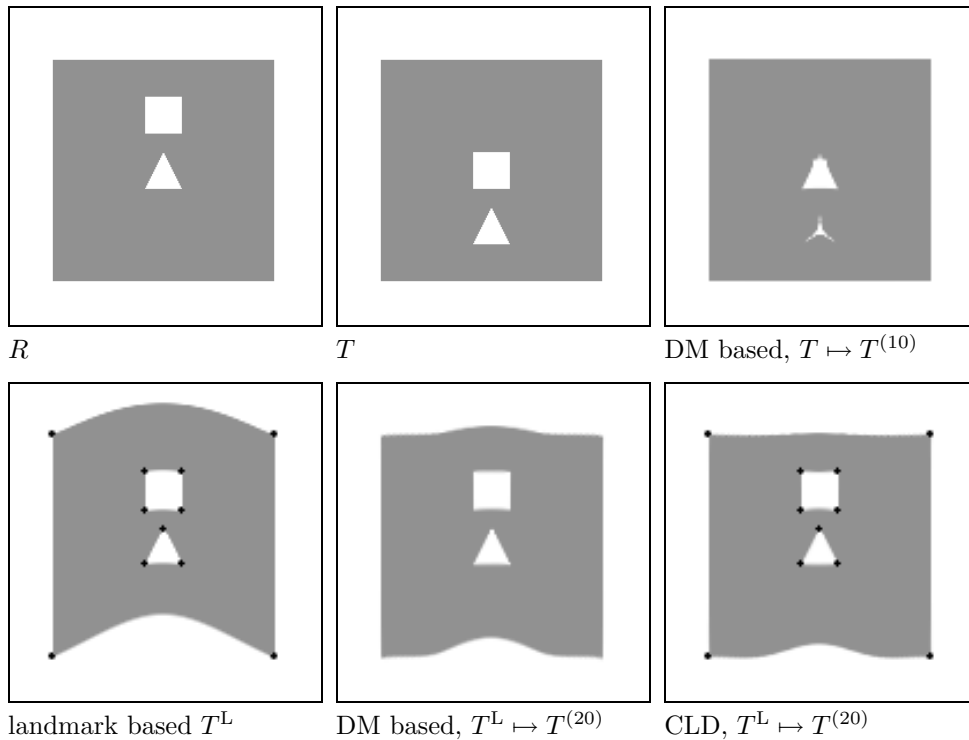


Figure 2: Registration results for the triangle example. TOP LEFT: reference  $R$ , TOP MIDDLE: template  $T$ , TOP RIGHT: intermediate result of a plain distance measure based (DM) registration (10th iterate), BOTTOM LEFT: result of a landmark based registration (overlaid with the eleven landmarks), BOTTOM MIDDLE: intermediate result of a plain distance measure based registration (20th iterate) using the outcome of the landmark registration as starting configuration, BOTTOM RIGHT: intermediate result of the CLG registration (20th iterate) using the outcome of the landmark registration as starting configuration (overlaid with the eleven landmarks).

display the 20th iterate. After about 50 iterations, the deformed template perfectly matches the reference.

Finally, the bottom right image displays the 20th iterate of the CLD approach. Again, after about 50 iterations, the deformed template perfectly matches the reference.

This example demonstrates that the information provided by additional landmarks may improve any distance measure based registration considerably. Note that a plain landmark based registration does not lead to a satisfactory registration. Also note, distance measure based registration has a strong tendency to map edges to edges and corners to corners. Thus, since the landmarks in this example are all located at corners, the differences between the third and fourth registration are minor.

## 5.2 Internal landmarks

In the second example, the reference is again a big gray square, now with an inner white disk in the top left corner, while in the template, a smaller disk is located in the bottom right corner; cf. Fig. 3. Note that an affine linear pre-registration would rotate the template image

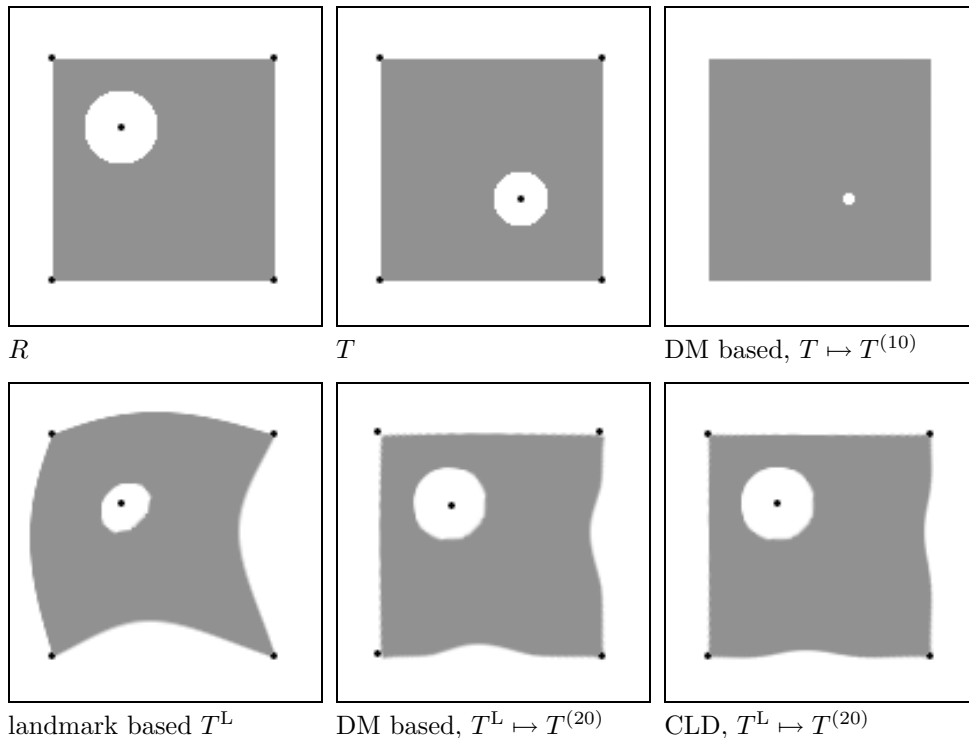


Figure 3: Registration results for the disk example. TOP LEFT: reference  $R$ , TOP MIDDLE: template  $T$ , TOP RIGHT: intermediate result of a plain distance measure (DM) based registration (10th iterate), BOTTOM LEFT: result of a landmark based registration (overlaid with the five landmarks), BOTTOM MIDDLE: intermediate result of a plain distance measure based registration (20th iterate) using the outcome of the landmark registration as starting configuration, BOTTOM RIGHT: intermediate result of the CLD registration (20th iterate) using the outcome of the landmark registration as starting configuration (overlaid with the five landmarks).

in order to map the two disks. As a consequence, the lower right corner of the square would be moved to the upper left position and thus would produce a miss-registration, assuming that corresponding corners of the big square should be matched onto each other.

Fig. 3 displays four registration results. The first one (top right image) shows an intermediate result of a plain distance measure based registration. Here, the inner disk has already been contracted considerably and will finally disappear.

The second registration (bottom left image) is a plain landmark based registration. As landmarks, we used the four corners of the square and the center of the disk. Note that the displayed landmarks (black “+” on gray background) do not belong to the images. As it is apparent from this figure, neither the inner disk nor the outer square have been matched sufficiently. In particular, the disk has been deformed such that the landmark is no longer in the center of the deformed disk.

The third registration (bottom middle image) is again a distance measure based registration, but now we used the result of the landmark based registration as a starting point. Here we show the 20th iterate. Note that the corners of the square as well as the center of the disk are slightly off. After about 50 iterations, the corners will be mapped onto the

corners of the reference image, however, the center of the disk remains off by about 2%.

Finally, in the bottom right image, we show the 20th iterate of the CLD approach, where again after about 50 iterations the result is a copy of the reference. Note that this time the position of the landmarks is fixed by construction. Thus, we are able to guarantee a one-to-one point match of corresponding landmarks.

This example demonstrates the difference between a distance measure based registration starting with a landmark based pre-registration and our CLD approach. As it turns out, distance measure based registration techniques do produce in general very good results. If in particular landmarks are located at edges or corners, the registration leads to an almost one-to-one relation of these landmarks. However, if landmarks are not related to edges or corners, landmarks can be miss-registered. The main point is, that in our CLD approach the correspondence of the landmarks is not by chance or just for specific landmarks. The new approach produces by construction a one-to-one correspondence, which can be guaranteed.

### 5.3 X-rays of human hands

Figure 4 displays the registration of X-rays of two human hands. These images are popular choice for testing registration schemes [1]. Again, the plain landmark based approach (middle left image) does produce a visually displeasing result. The result after curvature registration (top right image) looks perfect. However, a close examination shows that the landmarks are slightly off. Finally, we display several intermediate steps of the CLD scheme. It shows that not only the landmarks are perfectly matched but also the remaining part is nicely registered.

## 6 CONCLUSIONS

We have proposed a novel framework for parameter-free, non-rigid registration schemes which allows for the additional incorporation of user prescribed landmarks. The new CLD approach enhances the reliability of conventional approaches considerably and thereby their acceptability by practitioners in a clinical environment. Also, the new feature enables the user to incorporate pre-knowledge and thereby to guide the scheme to the desired solution.

It has been shown that the new CLD approach does compute a displacement field which is guaranteed to produce a one-to-one match between given landmarks and at the same time minimizes an intensity based measure for the remaining parts of the images. Moreover, its complexity is comparable to the ones for conventional registration schemes, which are not capable to incorporate additional landmark information.

We note that the new approach is easily extendable to incorporate other anatomic features like curves, crest lines, etc. Also, it is possible to substitute the interpolatory constraints by some approximation constraints, which soften at will the hard requirement that landmarks should be perfectly matched on top of each other. We will report on these approaches as well as on the application of our CLD scheme for the registration of high-resolution anatomical atlas of a human hip onto a low-resolution CT scan, needed for surgery planning, in a forthcoming paper.

The outlined framework is content of the patent AZ 102 53 784.4.

## References

- [1] Yali Amit, *A nonlinear variational problem for image matching*, SIAM J. Sci. Comput. **15** (1994), no. 1, 207–224.

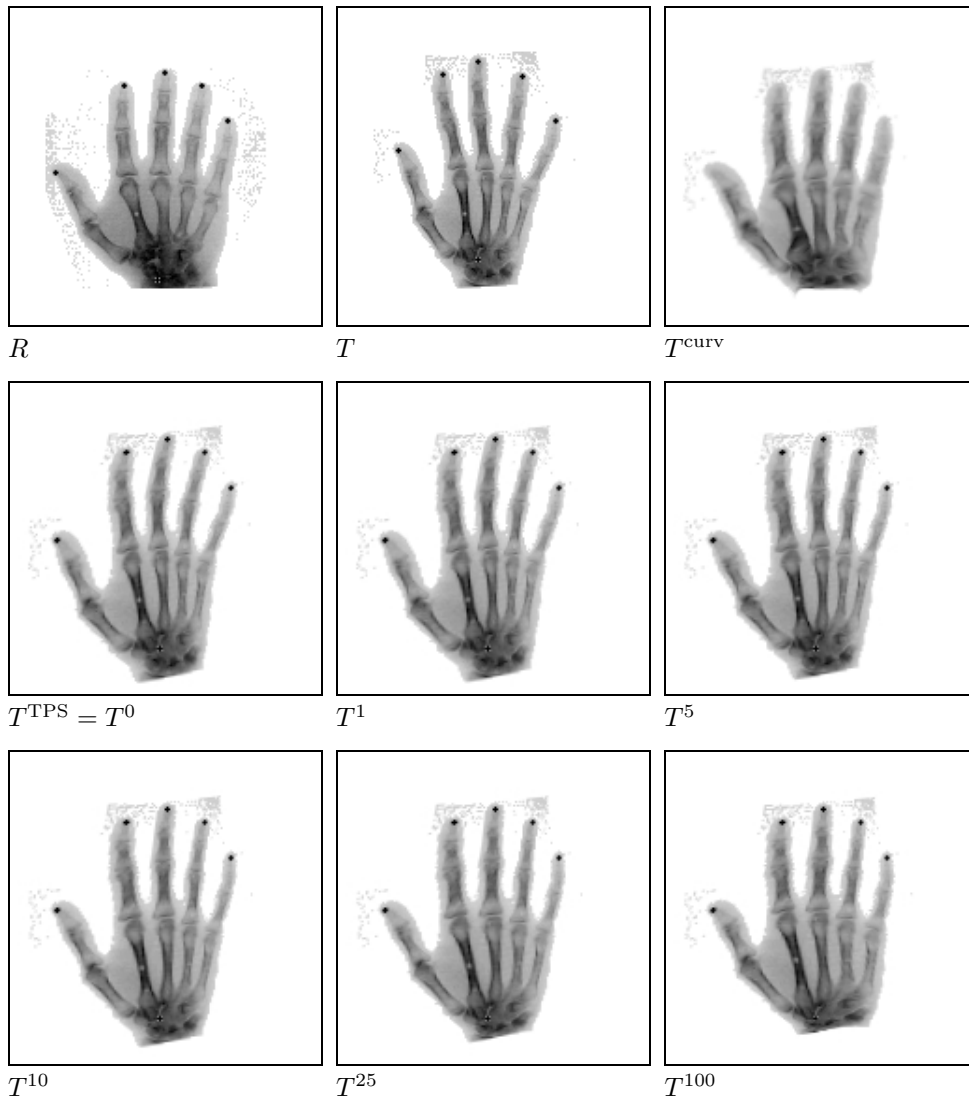


Figure 4: Registration results for X-rays of a human hand (images from Y. AMIT [1]): TOP LEFT: reference  $R$  (overlaid with six landmarks), TOP MIDDLE: template  $T$  (overlaid with 6 corresponding landmarks), TOP RIGHT: template  $T^{\text{curv}}$  after distance measure based registration (after 100 iterations),  $T^k$ ,  $k = 0, 1, 5, 10, 25, 100$  intermediate results of the CLD registration (overlaid with six corresponding landmarks).

- [2] Ruzena Bajcsy and Stane Kovačič, *Toward an individualized brain atlas elastic matching*, Tech. Report MS-CIS-86-71 Grasp Lap 76, Dept. of Computer and Information Science, Moore School, University of Philadelphia, 1986.
- [3] Fred L. Bookstein, *Principal warps: Thin-plate splines and the decomposition of deformations*, IEEE Transactions on Pattern Analysis and Machine Intelligence **11** (1989), no. 6, 567–585.
- [4] Morten Bro-Nielsen, *Medical image registration and surgery simulation*, Ph.D. thesis,

- IMM, Technical University of Denmark, 1996.
- [5] Chaim Broit, *Optimal registration of deformed images*, Ph.D. thesis, Computer and Information Science, Uni Pennsylvania, 1981.
  - [6] Lisa Gottesfeld Brown, *A survey of image registration techniques*, ACM Computing Surveys **24** (1992), no. 4, 325–376.
  - [7] Gary Edward Christensen, *Deformable shape models for anatomy*, Ph.D. thesis, Sever Institute of Technology, Washington University, 1994.
  - [8] A. Collignon, A. Vandermeulen, P. Suetens, and G. Marchal, *3d multi-modality medical image registration based on information theory*, Kluwer Academic Publishers: Computational Imaging and Vision **3** (1995), 263–274.
  - [9] Bernd Fischer and Jan Modersitzki, *Fast diffusion registration*, AMS Contemporary Mathematics, Inverse Problems, Image Analysis, and Medical Imaging, vol. 313, 2002, pp. 117–129.
  - [10] ———, *A unified approach to fast image registration and a new curvature based registration technique*, Preprint a-02-07, Institute of Mathematics, Medical University of Lübeck, 2002.
  - [11] ———, *Curvature based image registration*, JMIV **18** (2003), no. 1, 81–85.
  - [12] Pierre Hellier and Christian Barillot, *Coupling dense and landmark-based approaches for non rigid registration*, Tech. Report 1368, INRIA, France, 2000.
  - [13] Hans J. Johnson and Gary Edward Christensen, *Consistent landmark and intensity-based image registration*, IEEE Transactions on Medical Imaging **21** (2002), no. 5, 450–461.
  - [14] J. B. Antoine Maintz and Max A. Viergever, *A survey of medical image registration*, Medical Image Analysis **2** (1998), no. 1, 1–36.
  - [15] Calvin R. Maurer and J. Michael Fitzpatrick, *Interactive image-guided neurosurgery*, ch. A Review of Medical Image Registration, pp. 17–44, Park Ridge, IL, American Association of Neurological Surgeons, 1993.
  - [16] Jan Modersitzki, *Numerical methods for image registration*, Oxford University Press, to appear 2003.
  - [17] Karl Rohr, *Landmark-based image analysis*, Computational Imaging and Vision, Kluwer Academic Publishers, Dordrecht, 2001.
  - [18] Jean-Philippe Thirion, *Fast non-rigid matching of 3D medical images*, Tech. Report 2547, Institut National de Recherche en Informatique et en Automatique, France, may 1995.
  - [19] Petra A. van den Elsen, Evert-Jan D. Pol, and Max A. Viergever, *Medical image matching – a review with classification*, IEEE Engineering in Medicine and Biology (1993), 26–38.
  - [20] Paul A. Viola, *Alignment by maximization of mutual information*, Ph.D. thesis, Massachusetts Institute of Technology, june 1995, pp. 1–155.